Boundary Value Problems
a SpringerOpen Journal

RESEARCH Open Access

Complex potentials solutions for isotropic Cosserat bodies with voids

D.M. Neagu[1], I.M. Fudulu[1] and M. Marin[1,2*]

*Correspondence:
[1] Department of Mathematics and Computer Science, Transilvania University of Brasov, 500036 Brasov, Romania
[2] Academy of Romanian Scientists, Ilfov Street, No. 3, 050045 Bucharest, Romania

Abstract

This paper aims to obtain solutions in terms of the complex potential structure for the plain strain problem of an elastic micropolar and isotropic body with pores. The constitutive equations on which the method is applied and is useful are the well-known equations of the elasticity theory for the above-mentioned body. We intend to solve the Kirch problem using the procedure of complex variables.

Keywords: Cosserat media; Voids; Isotropic body; Plane problem; Complex potential

1 Introduction

The Cosserat brothers laid the foundations of a theory of the mechanics of continuous media in which, for each material point, we have the freedom degree of a rigid. Later, the theory of micropolar media was introduced and studied by Eringen [1–3] for material studies. Unlike the generalized continuous media theory (Cosserat brothers' theory) [4], which contains a conservation law for the microrotational inertia tensor, this theory considers three deformation directors. In this framework, the forces acting on the surface element are represented by the classic stress tensor and an additional couple tensor.

In this paper, we investigate plane strain within the equilibrium theory of micropolar, homogeneous, isotropic, and porous bodies. Using the constitutive equations (1)–(3), the geometric equations (4), and the equilibrium equations without body forces (5)–(7) from [5], we focus on addressing the fundamental boundary value problems of plane strain theory. Subsequently, we derive a depiction of the displacement of microrotations and pores using complex analytical functions and two real functions based on the homogeneous Helmholtz equations as described in [6]. In the fifth section, the structure of the potential functions for several domains of interest is studied, and in the sixth section, we apply the method of complex variables without introducing stress functions to solve the Kirch problem. The last section is dedicated to the numerical study, where we obtained the corresponding complex potential plots and stress and displacement distributions in a porous micropolar isotropic material. More studies on complex potentials can be found in [7, 8]. There also were countless studies aimed at the theory of micropolar media, among which we highlight [9–20].

2 Basic equations

We consider B a bounded domain from the three-dimensional Euclidean space, with ∂B as its boundary and n as the outer normal of the ∂B boundary. Assuming that we have a porous micropolar elastic medium occupying B, we associate the body with an orthogonal axis system $Ox_i(i = 1,2,3)$.

The basic equations describing the evolution of an isotropic Cosserat medium with voids are as follows.

The constitutive equations:

$$t_{ij} = \lambda u_{k,k}\delta_{ij} + \mu(u_{i,j} + u_{j,i}) + k(u_{i,j} + \varepsilon_{ijk}\phi_k) + \xi\varphi\delta_{ij}, \tag{1}$$

$$m_{ij} = \alpha\phi_{k,k}\delta_{ij} + \gamma\phi_{j,i} + \psi\phi_{i,j} + \zeta\varepsilon_{sji}\varphi_{,s}, \tag{2}$$

$$h_i = d\varphi_{,i}. \tag{3}$$

The geometrical relations:

$$e_{ij} = u_{i,j} + \varepsilon_{ijk}\phi_k, \quad \psi_{ij} = \phi_{i,j}. \tag{4}$$

Equilibrium equations (body loads are absent):

$$t_{ji,j} = 0, \tag{5}$$

$$m_{ji,j} + \varepsilon_{irs}t_{rs} = 0, \tag{6}$$

$$h_{i,i} + g = 0. \tag{7}$$

We consider:

$$t_i = t_{ji}n_j;\ m_i = m_{ji}n_j;\ N_i = h_{ji}n_j, \tag{8}$$

in which N_i is the generalized surface force at a regular point on ∂B, t_i is the surface force, and m_i is the surface moment.

We will further presume a positive quadratic form for the internal energy density from where we have

$$\begin{aligned}&\kappa > 0,\ \kappa + 2\mu > 0,\ \kappa + 2\mu + 3\lambda > 0, \quad d > 0,\\ &\gamma - \beta > 0,\ \gamma + \beta > 0,\ \gamma + \beta + 3\alpha > 0.\end{aligned} \tag{9}$$

3 Plane strain problem

In this part of the paper, we will consider B to be the interior of a right cylinder whose cross-section is Σ and whose lateral boundary is Π. This setup is related to an orthogonal coordinate system so that its generators are parallel to the x_3 axis. We denote by L the boundary corresponding to the cross-section. The plane strain is considered to be parallel to the x_1, x_2-plane. Therefore,

$$\begin{aligned}&u_\alpha = u_\alpha(x_1,x_2),\ u_3 = 0,\ \phi_\alpha = 0;\ \phi_3 = \phi(x_1,x_2),\\ &\varphi = \varphi(x_1,x_2), \quad (x_1,x_2) \in \Sigma.\end{aligned} \tag{10}$$

Taking these restrictions into account, from the constitutive equations and the geometric equations, we deduce that e_{ij}, ψ_{ij}, t_{ij}, m_{ij}, h_i are independent of x_3. So, taking into account that $t_{\alpha\beta}$, $m_{\alpha 3}$, t_{33}, $m_{3\alpha}$ and h_α are nonzero, the constitutive equations become:

$$t_{\alpha\beta} = \lambda u_{\rho,\rho}\delta_{\alpha\beta} + \mu(u_{\alpha,\beta} + u_{\beta,\alpha}) + \kappa(u_{\alpha,\beta} + \epsilon_{3\alpha\beta}\phi_\kappa) + \xi\varphi\delta_{\alpha\beta}, \tag{11}$$

$$m_{\alpha 3} = \psi\phi_{,\alpha} + \zeta\varepsilon_{3\beta\alpha}\varphi, \tag{12}$$

$$h_i = d\varphi_{,\alpha}. \tag{13}$$

From (4) and (10) it follows that the nonzero measures of plane deformation are:

$$e_{\alpha\beta} = u_{\beta,\alpha} + \varepsilon_{\beta\alpha 3}\phi, \quad \psi_{\alpha 3} = \phi_{,\alpha}. \tag{14}$$

Moreover, the equilibrium equations take the following form:

$$t_{\beta\alpha,\beta} = 0, \tag{15}$$

$$m_{\alpha 3,\alpha} + \varepsilon_{3\alpha\beta}t_{\alpha\beta} = 0, \tag{16}$$

$$h_{\alpha,\alpha} + g = 0 \text{ on } \Sigma. \tag{17}$$

For the vector t_i for the surface force, the vector m_i for the surface force couple, and the vector N_i for the void evolution at an ordinary point on L, we have:

$$t_\alpha = t_{\beta\alpha}n_\beta, \ \ m = m_{\rho 3}n_\rho, \ N = h_\alpha n_\alpha. \tag{18}$$

We will add the boundary conditions to the basic equations so that the first boundary problem is characterized by

$$u_\alpha = \tilde{u}_\alpha, \ \phi = \tilde{\phi}, \ \varphi = \tilde{\varphi} \text{ on } L \tag{19}$$

and the second by

$$t_{\beta\alpha}n_\beta = \tilde{t}_\alpha, m_{\alpha 3}n_\alpha = \tilde{m}, h_\alpha n_\alpha = \tilde{N} \text{ on } L, \tag{20}$$

where $\tilde{u}_\alpha$, $\tilde{\phi}$, $\tilde{\varphi}$ are prescribed functions, and $\tilde{t}_\alpha$, $\tilde{m}$, $\tilde{N}$ are given.

From (11)–(17), we get the system below, in terms of displacement, microrotation and pores. (Δ is the Laplacian)

$$\begin{aligned} &(\lambda + \mu)u_{\rho,\rho\alpha} + (\mu + \kappa)\Delta u_\alpha + \xi\varphi_{,\alpha} + \kappa\varepsilon_{3\alpha\beta}\phi_{,beta} = 0, \\ &\psi\Delta\varphi + \kappa\varepsilon_{3\alpha\beta}u_{\beta,\alpha} - 2k\phi = 0, \\ &d\Delta\varphi - \xi u_{\rho,\rho} - a\varphi = 0. \end{aligned} \tag{21}$$

More detailed steps to obtain the system can be found in [7].

4 Complex potentials

In this section, we will work in system (21) whose relations will be written in complex coordinates and integrated directly. In other words, we will determine the displacement using a pair of complex analytical functions, the microrotation, and the change in volume fraction in real functions verifying the homogeneous Helmholtz equations [6]. First, we introduce the complex coordinates

$$z = x_1 + ix_2, \overline{z} = x_1 - ix_2, \tag{22}$$

and complex displacement

$$U = u_1 + iu_2. \tag{23}$$

So, we get

$$\Delta = 4\frac{\partial^2}{\partial z \partial \overline{z}};\ u_{\rho,\rho} = \frac{\partial U}{\partial z} + \frac{\partial \overline{U}}{\partial \overline{z}};\ \varepsilon_{3\alpha\beta} u_{\beta,\alpha} = i\Big(\frac{\partial \overline{U}}{\partial \overline{z}} - \frac{\partial U}{\partial z}\Big). \tag{24}$$

Taking into account (24), we will rewrite the relations of system (21) in the following form:

$$\begin{aligned} &2(\kappa + \mu)\frac{\partial^2 U}{\partial z \partial \overline{z}} + (\mu + \lambda)\frac{\partial}{\partial \overline{z}}\Big(\frac{\partial U}{\partial z} + \frac{\partial \overline{U}}{\partial \overline{z}}\Big) + \xi\frac{\partial \varphi}{\partial \overline{z}} - i\kappa\frac{\partial \phi}{\partial \overline{z}} = 0,\\ &4\psi\frac{\partial^2 \phi}{\partial z \partial \overline{z}} - i\kappa\Big(\frac{\partial U}{\partial z} - \frac{\partial \overline{U}}{\partial \overline{z}}\Big) - 2\kappa\phi = 0,\\ &4d\frac{\partial^2 \varphi}{\partial z \partial \overline{z}} - \xi\Big(\frac{\partial U}{\partial z} + \frac{\partial \overline{U}}{\partial \overline{z}}\Big) - a\varphi = 0. \end{aligned} \tag{25}$$

We integrate the first relation of this system to obtain

$$2(\mu + \kappa)\frac{\partial U}{\partial z} + (\lambda + \mu)\Big(\frac{\partial U}{\partial z} + \frac{\partial \overline{U}}{\partial \overline{z}}\Big) + \xi\varphi - i\kappa\phi = \Gamma'(z), \tag{26}$$

where Γ is a complex analytic function on z, and $d\Gamma'(z) = \frac{d\Gamma(z)}{dz}$.

By conjugation of relation (26), we get

$$2(\mu + \kappa)\frac{\partial \overline{U}}{\partial z} + (\lambda + \mu)\Big(\frac{\partial U}{\partial z} + \frac{\partial \overline{U}}{\partial \overline{z}}\Big) + \xi\varphi + i\kappa\phi = \overline{\Gamma}'(z). \tag{27}$$

Next, using the relations (26) and (27), we get by summing the relation

$$\frac{\partial U}{\partial z} + \frac{\partial \overline{U}}{\partial \overline{z}} = \frac{1}{2(2\mu + \kappa + \lambda)}[\Gamma'(z) + \overline{\Gamma}'(\overline{z}) - 2\xi\varphi], \tag{28}$$

and by subtraction the relation

$$\frac{\partial U}{\partial z} - \frac{\partial \overline{U}}{\partial \overline{z}} = \frac{1}{2(\mu + \kappa)}[\Gamma'(z) - \overline{\Gamma}'(\overline{z}) + 2i\kappa\phi(z, \overline{z})]. \tag{29}$$

From the third relation of system (25) and from (28), we deduce that

$$\left(4\frac{\partial^2}{\partial z\partial\overline{z}} - m^2\right)\varphi = \frac{\xi}{2d(2\mu+\kappa+\lambda)}[\Gamma(z) + \overline{\Gamma}'(\overline{z})], \tag{30}$$

where

$$m = \frac{a(2\mu+\kappa+\lambda) - \xi^2}{d(2\mu+\kappa+\lambda)},$$

with $m^2 > 0$, according to (9). Therefore, we deduce that the function φ can be written in the form

$$\varphi = M - \frac{\xi}{2dm^2(2\mu+\kappa+\lambda)}[\Gamma(z) + \overline{\Gamma}'(\overline{z})], \tag{31}$$

where M is a real function that satisfies

$$\left(4\frac{\partial^2}{\partial z\partial\overline{z}} - m^2\right)M = 0. \tag{32}$$

Taking into account (28) and (31), we find:

$$\frac{\partial U}{\partial z} + \frac{\partial\overline{U}}{\partial z} = R[\Gamma'(z) + \overline{\Gamma}'(\overline{z})] - \frac{\xi}{2\mu+\kappa+\lambda}M, \tag{33}$$

where

$$R = \frac{\xi + dm^2(2\mu+\kappa+\lambda)}{2dm^2(2\mu+\kappa+\lambda)}.$$

Next, considering the second equation of system (25) and relation (29), we obtain

$$\left(4\frac{\partial^2}{\partial z\partial\overline{z}} - p^2\right)\phi = \frac{i\kappa}{2\gamma(\mu+\kappa)}[\Gamma'(z) - \overline{\Gamma}'(\overline{z})], \tag{34}$$

where

$$p^2 = \frac{\kappa(2\mu+\kappa)}{\psi(\mu+\kappa)}.$$

The ϕ function can be rewritten as follows:

$$\phi = P - \frac{i\kappa}{2\gamma p^2(\mu+\kappa)}[\Gamma'(z) - \overline{\Gamma}'(\overline{z})], \tag{35}$$

where the real function P satisfies

$$\left(4\frac{\partial^2}{\partial z\partial\overline{z}} - p^2\right)P = 0. \tag{36}$$

From (27), (31)–(33), and (36), we deduce that

$$\frac{\partial U}{\partial z} = \eta_1\Gamma'(z) - \eta_2\overline{\Gamma}'(\overline{z}) + 4iq_1\frac{\partial^2 P}{\partial z\partial\overline{z}} - 4q_2\frac{\partial^2 M}{\partial z\partial\overline{z}}, \tag{37}$$

where we denoted by η_1, η_2, q_1 and q_2 the following:

$$\eta_1 = \frac{3\mu + \lambda + 2\kappa}{4(\mu + k)(2\mu + \lambda + \kappa)} + \frac{\kappa}{4(2\mu + \kappa)(\mu + \kappa)} + \frac{\xi^2}{4dm^2(2\mu + \lambda + \kappa)^2},$$
$$\eta_2 = \frac{\mu + \lambda}{4(\mu + k)(2\mu + \lambda + \kappa)} + \frac{\kappa}{4(2\mu + \kappa)(\mu + \kappa)} - \frac{\xi^2}{4dm^2(2\mu + \lambda + \kappa)^2},$$
$$q_1 = \frac{\kappa}{2p^2(\mu + \kappa)}, \ q_2 = \frac{\xi}{2m^2(2\mu + \lambda + \kappa)}.$$

Let ω be a complex analytic function on z. By integrating equation (37), we get

$$U = \eta_1 \Gamma(z) - \eta_2 \overline{\Gamma}(\overline{z}) z - \overline{\omega}(\overline{z}) + 4iq_1 \frac{\partial P}{\partial z} - 4q_2 \frac{\partial M}{\partial \overline{z}}. \tag{38}$$

Previously, we were able to obtain in relations (31), (35), and (38) a representation of the functions φ, ϕ and U in terms of the analytic complex functions Γ, ω and the real functions M and P.

Next, following some simple calculations, we deduce the equalities below:

$$\begin{aligned}
&t_{11} + t_{22} = 2\xi\varphi + (2\lambda + 2\mu + \kappa) u_{\rho,\rho},\\
&t_{11} + it_{12} - t_{22} + it_{21} = (\kappa + 2\mu)[u_{1,1} + iu_{1,2} - u_{2,2} + iu_{2,1}] = 2(2\mu + \kappa)\frac{\partial U}{\partial \overline{z}},\\
&t_{21} - t_{12} = (u_{2,1} - u_{1,2} - 2\phi)\kappa,\\
&m_{13} - im_{23} = 2\psi \frac{\partial \phi}{\partial z} - i\zeta \frac{\partial \varphi}{\partial z},\\
&h_1 - ih_2 = 2d \frac{\partial \varphi}{\partial z}.
\end{aligned} \tag{39}$$

Using (24), (34), (36), and (39), we obtain the following form of the relations presented in the previous system:

$$\begin{aligned}
&t_{11} + t_{22} = \frac{a(2\mu + 2\lambda + \kappa) - 2\xi^2}{2dm^2(2\mu + \kappa + \lambda)}[\Gamma'(x) + \overline{\Gamma}'(\overline{z})] + \frac{\xi(2\mu + \kappa)}{2\mu + \kappa + \lambda} M,\\
&t_{11} + it_{12} - t_{22} + it_{21} = -2(2\mu + k)\Big[\eta_2 \overline{\Gamma}''(\overline{z}) z + \overline{\omega}(\overline{z}) - 4iq_1 \frac{\partial^2 P}{\partial \overline{z}^2} + 4q_2 \frac{\partial^2 M}{\partial \overline{z}^2}\Big],\\
&t_{21} - t_{12} = \gamma p^2 P,\\
&m_{13} - im_{23} = 2\gamma \frac{\partial P}{\partial z} + 2i\zeta \frac{\partial M}{\partial z} - i\Big[\frac{\kappa}{p^2(\mu + \kappa)} + \frac{\zeta\xi}{dm^2(2\mu + \lambda + \kappa)}\Big]\Gamma''(z),\\
&h_1 - ih_2 = 2d \frac{\partial M}{\partial z} - \frac{\xi}{m^2(2\mu + \lambda + \kappa)}\Gamma''(z).
\end{aligned} \tag{40}$$

Next, we will use the following relations:

$$n_1 = -\frac{1}{2} i \Big(\frac{dz}{ds} - \frac{d\overline{z}}{ds}\Big), \quad n_2 = -\frac{1}{2}\Big(\frac{dz}{ds} + \frac{d\overline{z}}{ds}\Big),$$

considering that L is a smooth piecewise arclength-parameterized curve. From (20), we have

$$
\begin{aligned}
&t_1 + it_2 = \frac{1}{2}[t_{12} - it_{11} - t_{21} - it_{22}]\frac{dz}{ds} + i\frac{1}{2}[t_{11} + it_{12} - t_{22} + it_{21}]\frac{d\overline{z}}{ds},\\
&m = Im\{(m_{13} - im_{23}\frac{dz}{ds}\},\\
&h = Im\{(h_1 - ih_2)\frac{dz}{ds}\},
\end{aligned}
\tag{41}
$$

where $Im\{\}$ represents the imaginary part of $\{\}$. We note that

$$
t_{11} + t_{22} = 2(2\mu + k)\{\eta_2[\Gamma'(z) + \overline{\Gamma}'(\overline{z})] + q_2 m^2 M\}. \tag{42}
$$

Using (40)–(42), we get

$$
\begin{aligned}
&t_1 + it_2 = -(2\mu + \kappa)i\frac{d}{ds}\{\eta_2[\Gamma(z) + z\overline{\Gamma}'(\overline{z})] + \overline{\omega}(\overline{z}) - 4iq_1\frac{\partial P}{\partial \overline{z}} + 4q_2\frac{\partial M}{\partial \overline{z}}\},\\
&m = Im\{2\gamma\frac{\partial P}{\partial z} + 2i\zeta\frac{\partial M}{\partial z} - iw_1\Gamma''(z)]\frac{dz}{ds}\},\\
&h = Im\{[2d\frac{\partial M}{\partial z} - w_2\Gamma''(z)]\frac{dz}{ds}\},
\end{aligned}
\tag{43}
$$

where we used the following notations:

$$
w_1 = \frac{\kappa}{p^2(\mu + \kappa)} + \frac{\zeta\xi}{dm^2(2\mu + \lambda + \kappa)}; \quad w_2 = \frac{\xi}{m^2(2\mu + \lambda + \kappa)}.
$$

We use the notations S_1 and S_2 for the vector components resulting from the application of external stresses to the contour L. Hence, we get

$$
S_1 + iS_2 = \int_L (t_1 + it_2)ds = -(2\mu + \kappa)i\{\eta_2[\Gamma(z) + z\overline{\Gamma}'(\overline{z})] + \overline{\omega}(\overline{z}) - 4iq_1\frac{\partial P}{\partial \overline{z}} + 4q_2\frac{\partial M}{\partial \overline{z}}\}_A^A. \tag{44}
$$

A function F changes its value when moving around the contour L in the conventional positive direction. For one round, we denote these changes by $\{F\}_A^A$.

Now, we can express the boundary conditions (19) in the following form:

$$
\begin{aligned}
&\eta_1\Gamma(z) - \eta_2 x\overline{\Gamma}'(\overline{z}) - \overline{\omega}(\overline{z}) + 4iq_1\frac{\partial P}{\partial \overline{z}} - 4q_2\frac{\partial M}{\partial \overline{z}} = \tilde{u}(s),\\
&P(z,\overline{z}) - \frac{i\kappa}{2\gamma p^2(\kappa + \mu)}[\Gamma'(z) - \overline{\Gamma}'(\overline{z})] = \phi(s),\\
&M(z,\overline{z}) - \frac{\xi}{2dm^2(2\mu + \lambda + \kappa)}[\Gamma(z) + \overline{\Gamma}'(\overline{z})] = \varphi(s), \ z \in L,
\end{aligned}
\tag{45}
$$

where $\tilde{u} = \tilde{u}_1 + i\tilde{u}_2$. Moreover, from (43), the boundary conditions (20) can take the following form:

$$
(2\mu + \kappa)\frac{d}{ds}\{\eta_2[\Gamma(z) + z\overline{\Gamma}'(\overline{z})] + \overline{\omega}(\overline{z}) - 4iq_1\frac{\partial P}{\partial \overline{z}} + 4q_2\frac{\partial M}{\partial \overline{z}}\} = \tilde{t}(s),
$$

$$Im\{[2\gamma\frac{\partial P}{\partial z}+2i\zeta\frac{\partial M}{\partial z}-iw_1\Gamma''(z)]\frac{dz}{ds}\}=\tilde{m}(s),$$
$$Im\{[2d\frac{\partial M}{\partial z}-w_2\Gamma''(z)]\frac{dz}{ds}\}=\tilde{N}(s),z\in L,\qquad(46)$$

where $\tilde{t}(s)=i(\tilde{t}_1+i\tilde{t}_2)$.

5 Construction of potentials

In this section, we aim to derive the structure of the potentials Γ, ω, P, and M and to explore their arbitrariness across various domains of interest. We analyze the differences between the configurations of the following sets of potentials (Γ,ω,P,M) and $(\Gamma^*,\omega^*,P^*,M^*)$, corresponding to the same functions $t_{\alpha\beta}$, $m_{\alpha 3}$ and h_α.

According to (40), it is required that

$$Re[\Gamma'(z)]=Re[\Gamma^{*'}(z)],\quad M=M^*,\quad P=P^*,$$
$$\eta_2 z\overline{\Gamma}''(\overline{z})+\overline{\omega}'(\overline{z})=\eta_2 z\overline{\Gamma}^{*''}(\overline{z})+\overline{\omega}^{*'}(\overline{z}),$$

where $Re[]$ denotes the real part of []. Therefore, we deduce that

$$\begin{aligned}&\Gamma(z)=\Gamma^*(z)+iX_z+\rho_1,\\&\omega(z)=\omega^*(z)+\rho_2,\\&P=P^*,\\&M=M^*,\end{aligned}\qquad(47)$$

where X is a real constant, and ρ_1, ρ_2 are complex constants.

We can set the origin of the coordinates in Σ such that X, ρ_1, ρ_2 satisfy the conditions

$$\Gamma(0)=0,\ Im\{\Gamma'(0)\}=0,\omega(0)=0,\qquad(48)$$

which ensure the unique determination of Γ and ω.

We consider that (Γ,ω,P,M) and $(\Gamma^*,\omega^*,P^*,M^*)$ are correlated with u_α, ϕ_α and φ, which indicates that we cannot have a greater arbitrariness than in (46). Referring to relation (39), the displacement imposes $X=0$ and $\eta_1\rho_1=\overline{\rho}_2$. Consequently, we can select ρ_1 such that $\Gamma(0)=0$.

Given that Γ and ω are single-valued and analytic functions within a bounded, simply connected region, we focus on the situation where the cross section is bounded and multiple connected. We will consider the boundary L as comprising $(m+1)$ simple and closed L_j contours, ensuring L_{m+1} encompasses all L_k contours (where $(k=1,2,\dots,m)$).

Assuming that u_α, ϕ_α, φ and the stress functions $t_{\alpha,\beta}$, $m_{\alpha,\beta}$ and h_α have a unique value and from (40), we deduce that M, P and their second-order derivatives must also be single-valued. From this, we derive the following form of the complex potentials:

$$\begin{aligned}&\Gamma(z)=\sum_{k=1}^{m}(zX_k+Y_k)log(z-z_k)+\Gamma_1(z),\\&\omega(z)=\sum_{k=1}^{m}Z_k log(z-z_k)+\omega_1(z),\end{aligned}\qquad(49)$$

where z_k represents a point in the simply connected region Σ_k bounded by L_k, Γ_1, and ω_1 are single-valued analytic functions on Σ, Y_k and Z_k are complex constants, and A_k are real constants. Therefore, from (31), (35), (38), and (48), we deduce that

$$[U]_{L_k} = 2\pi[(\eta_1 + \eta_2)zX_k + \eta_1 Y_k + \overline{Z}_k],$$
$$[\phi]_{L_k} = 2\pi(\eta_1 + \eta_2)zX_k,$$
$$[\varphi]_{L_k} = 0.$$

Here, the notation $[]_{L_k}$ represents the change in the value of the function when surrounding the contour L_k once in the conventional positive sense. Taking into account the fact that u_α and ϕ_α must have unique values, we deduce the following conditions:

$$X_k = 0, \quad \eta_1 Y_k + \overline{Z}_k = 0. \tag{50}$$

We denote the resultant of the stress vector applied to the contour as $S_1^{(k)}$, $S_2^{(k)}$. Based on equations (43), (44), and (48), we derive

$$S_1^{(k)} + iS_2^{(k)} = -2\pi(2\mu + \kappa)(\eta_2 Y_k - \overline{Z}_k). \tag{51}$$

From (50) and (51), it follows that

$$Y_k = -\frac{1}{2\pi}(S_1^{(k)} + iS_2^{(k)}); \quad Z_k = -\eta_1 \overline{Y}_k. \tag{52}$$

Therefore, from (49), we get

$$\begin{aligned} \Gamma(z) &= -\frac{1}{2\pi}\sum_{k=1}^{n}(S_1^{(k)} + iS_2^{(k)})log(z - z_k) + \Gamma_1(z), \\ \omega(z) &= \frac{1}{2\pi}\eta_1\sum_{k=1}^{m}(S_1^{(k)} - iS_2^{(k)})log(z - z_k) + \omega_1(z). \end{aligned} \tag{53}$$

In the study of complex analysis and potential theory, unbounded domains and the behavior of functions at infinity play a crucial role. Theorem 1, stated below, provides significant insights into the behavior of functions defined on such domains, particularly in terms of their integral representations and asymptotic properties.

Theorem 1 *Let Σ be an unbounded domain with the outlines δ_1, δ_2, ..., δ_m as internal bounded regions. Assuming the origin $z = 0$ is exterior to Σ and h_α, $t_{\alpha\beta}$, and $m_{\alpha\beta}$ are delimited in the vicinity of the limit point and for $|z| = \chi$ sufficiently large, we have*

$$\begin{aligned} \Gamma(z) &= -\frac{1}{2\pi}(R_1 + iR_2)logz + (a_1 + ia_2)z + \Gamma_0(z), \\ \omega(z) &= \frac{1}{2\pi}\eta_1(R_1 - iR_2)logz + (b_1 + ib_2)z + \omega_0(z), \\ P(z,\overline{z}) &= \sum_{n=0}^{\infty}(P_n e^{in\theta} + \overline{P}_n e^{-in\theta})K_n(\tau\chi), \end{aligned} \tag{54}$$

$$M(z,\overline{z}) = \sum_{n=0}^{\infty}(M_n e^{in\theta} + \overline{M}_n e^{-n\theta})K_n(w\chi).$$

In the previous theorem, Γ_0 and ω_0 represent single-valued analytic functions on Σ including the limit at infinity, and we used the notations a_α and b_α for real constants, P_n and M_n for complex constants, K_n for modified Bessel functions of order n and

$$R_\alpha = \sum_{k=1}^{m} S_\alpha^{(k)}; \quad z = re^{i\theta}. \tag{55}$$

For sufficiently large $|z|$, we can express the functions Γ_0 and ω_0 in the following form:

$$\Gamma_0 = \sum_{n=0}^{\infty} D_n z^{-n}, \quad \omega_0(z) = \sum_{n=0}^{\infty} E_n z^{-n}. \tag{56}$$

We consider that

$$\lim_{P\to\infty} t_{\alpha\beta}(P) = t^*_{\alpha\beta}.$$

From (40), (42), and (53), it follows that

$$\begin{aligned} t^*_{11} &= (2\mu + \kappa)(2\eta_2 a_1 - b_1), \\ t^*_{22} &= (2\mu + \kappa)(2\eta_2 a_1 + b_1), \\ t^*_{12} &= t^*_{21} = (2\mu + \kappa)b_2. \end{aligned} \tag{57}$$

The constant b_2 depends on the rigid rotation at infinity ϵ via

$$a_2 = (2\mu + \kappa)\varepsilon. \tag{58}$$

6 The stress that occurs around the hole

In this part of the paper, we will use the results obtained in the previous sections. Using boundary conditions and complex potentials, the following theorem allows the analysis of stress and deformation of materials with circular inclusions under external load conditions.

Theorem 2 *Let $\Sigma_1 = \{(x_1, x_2) \in \mathbb{R}^2, x_1^2 + x_2^2 > \chi^2\}$ be an unbounded domain with a circular hole centered at the origin and with radius χ. Assuming that an axial uniform stress acts on the body in the x_1 direction, at infinity, we have*:

$$t^*_{11} = Q, \;\; t^*_{12} = t^*_{21} = t^*_{22} = 0, \;\; m^*_{\alpha 3} = 0, h^*_\alpha = 0, \tag{59}$$

where Q is a given constant.

At the boundary of the hole, we have

$$\eta_2[\Gamma(z) + z\overline{\Gamma}'(\overline{z})] + \overline{\omega}(\overline{z}) - 4iq_1\frac{\partial P}{\partial \overline{z}} + 4q_2\frac{\partial M}{\partial \overline{z}} = 0,$$

$$Im\{[2\gamma\frac{\partial P}{\partial z} - iw_1\Gamma''(z)]\frac{dz}{ds}\} = 0,$$
$$Im\{[2d\frac{\partial M}{\partial z} - w_2\Gamma''(z)]\frac{dz}{ds}\} = 0, \ for \ |z| = \chi, \tag{60}$$

where the components of the complex potentials are as follows:

$$\Gamma(z) = \frac{1}{4\eta_2(2\mu+\kappa)}Qz + \frac{1}{z}D_1,$$
$$\omega(z) = -\frac{1}{2(2\mu+\kappa)}Qz + \frac{1}{z}E_1 + \frac{1}{z^3}E_3, \tag{61}$$
$$P(z,\overline{z}) = iH_1\Big(\frac{z}{\overline{z}} - \frac{\overline{z}}{z}\Big)K_2(\tau\chi),$$
$$M(z,\overline{z}) = H_2\Big(\frac{z}{\overline{z}} + \frac{\overline{z}}{z}\Big)K_2(w\chi), \quad \chi = (z\overline{z})^{1/2},$$

where

$$D_1 = \frac{1}{2(2\mu+\kappa)F}Q\xi^2, \quad E_1 = -\frac{1}{2(2\mu+\kappa)}Q\chi^2,$$
$$E_3 = \frac{1}{2(2\mu+\kappa)F}[\eta_2 + 1q_1\chi\tau TK_3(\tau\chi) + 2q_2\chi mHK_3(m\chi),$$
$$H_1 = TD_1, \ H_2 = HD_1, \ F = \eta_2 + 2q_1\tau a_2 TK_1(\tau\chi) + 2q_2 m\chi K_3(m\chi), \tag{62}$$
$$T = \frac{4}{2\chi^4\omega}\{8dK_2(m\chi) + 2m\chi\xi[K_1(m\chi) + K_3(\tau\chi)]\},$$
$$H = \frac{4}{3\chi^4\omega}\{8\gamma K_2(\tau\chi) - 2\tau\chi\xi[K_1(\tau\chi) + K_3(\tau\chi)]\},$$
$$\Omega = \frac{16d\gamma}{\chi^2}K_2(\tau\chi)K_2(m\chi) + 4m\tau\xi^2[K_1(m\chi) + K_3(m\chi)][K_1(\tau\chi) + K_3(\tau\chi)].$$

We note that R_1 and R_2 are 0, and in the case of stress analysis, we can consider that a_2, D_0, E_0. From (57) and (59), we find that

$$a_1 = \frac{1}{4\eta_2(2\mu+\kappa)}Q, \quad b_1 = -\frac{1}{2(2\mu+\kappa)}Q, \quad b_2 = 0. \tag{63}$$

In this case, the solution has the forms (54) and (56). Using them and (60), we get

$$e^{i\theta}U = u_\chi + iu_\theta,$$

where the components u_χ and u_θ are in polar coordinates. From (31), (35), (38), and (63), it follows that

$$u_\chi + iu_\theta = \frac{\eta_1 - \eta_2}{4\eta_2(2\mu+\kappa)}Q\chi - \frac{1}{\chi}(E_1 - \eta_1 D_1) + ucos2\theta + ivsin2\theta,$$
$$\phi = -2[H_1K_2(\tau\chi) - \frac{\kappa}{2\gamma\tau^2(\mu+\kappa)\chi^2}D_1]sin2\theta,$$
$$\varphi = -\frac{\xi Q}{4dm^2\eta_2(2\mu+\lambda+\kappa)(2\mu+\kappa)} + 2[H_2K_2(m\chi) + \frac{\xi}{2dm^2(2\mu+\lambda+\kappa)\chi^2}]cos2\theta,$$

where

$$u = \frac{1}{\chi}\eta_2 D_1 + \frac{Q\chi}{2(2\mu+\kappa)} - \frac{1}{\chi^3}E_3 + \frac{2}{\chi}q_1 H_1 K_2(\tau\chi) + 2mq_2 H_2[K_1(m\chi) + K_3(m\chi)],$$
$$v = \frac{1}{\chi}\eta_2 D_1 - \frac{Q\chi}{2(2\mu+\kappa)} - \frac{1}{r^3}E_3 + 2q_1 H_1[K_1(\tau\chi) + K_3(\tau\chi)] + \frac{8}{rq_2}H_2 K_2(m\chi).$$

Similarly, using (40) and (62), we obtain the stresses.

7 Numerical simulation

The graphs below (Figs. 1–4) correspond to an isotropic magnesium crystal with pores and are obtained using the "Wolfram Mathematica" computing system. The values used can be found in [9]. The acquired plots represent the real and imaginary parts of the $\Gamma(z)$ and $\omega(z)$ potentials, which can be found in Sect. 5. These allow us to visualize the variation of potentials in the complex. More precisely, these graphs help to understand the stress and displacement fields in the material, identify critical regions, and predict the behavior of the material under various conditions.

In the representation, $Im(\Gamma(z))$, a peak located in the center can be observed, which indicates a region where the imaginary part has a significant value. This may be due to stress concentration or a singularity in the material. In both representations, flat regions suggest slow changes in those areas. There is a visible central valley in the $Re(\Gamma(z))$ representation, which indicates a negative value and may suggest comprehensive stresses or regions of low potential.

Regarding the corresponding plots of $Re(\omega(z))$ and $Im(\omega(z))$, peaks and valleys can also be observed, indicating peaks of maximum and minimum displacement. Microrotations affect the displacement and strain fields, leading to more complex patterns in the graphics. Sharp peaks suggest the presence of singularities or displacement concentration points, possibly near pores or defects in the material. These plots help to understand the displacement and strain fields in the material, identify critical regions, and predict the behavior of the material under various conditions.

The following four graphs correspond to the imaginary and real parts of the radial displacement component "u" and the tangential displacement component "v" of Sect. 6. The

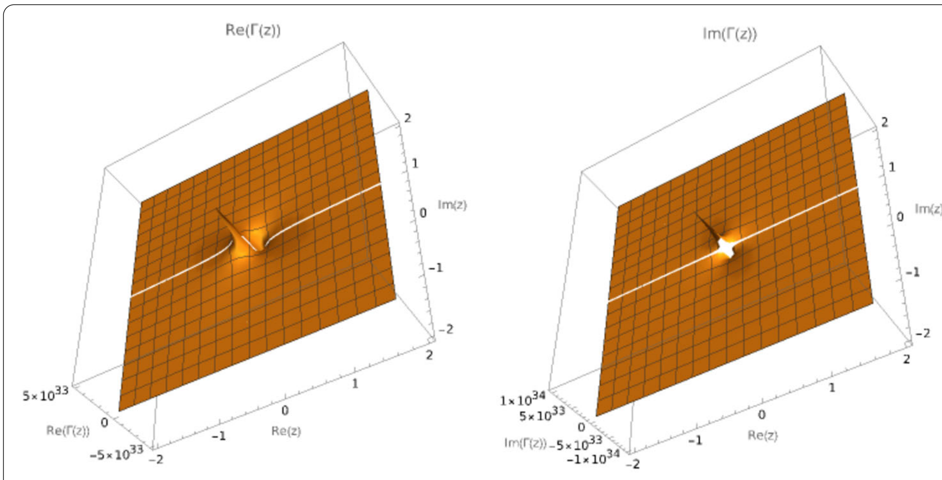

Figure 1 The behavior of $Re(\Gamma(z))$ and $Im(\Gamma(z))$

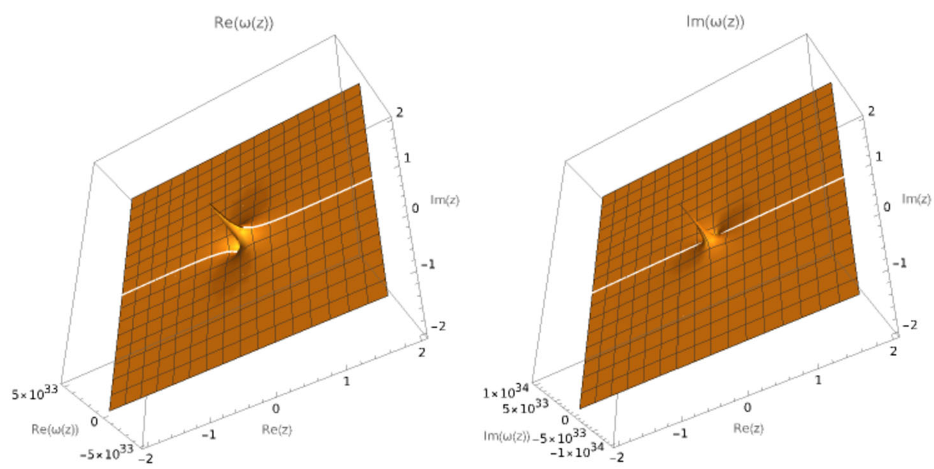

Figure 2 The behavior of *Re*(ω(*z*)) and *Im*(ω(*z*))

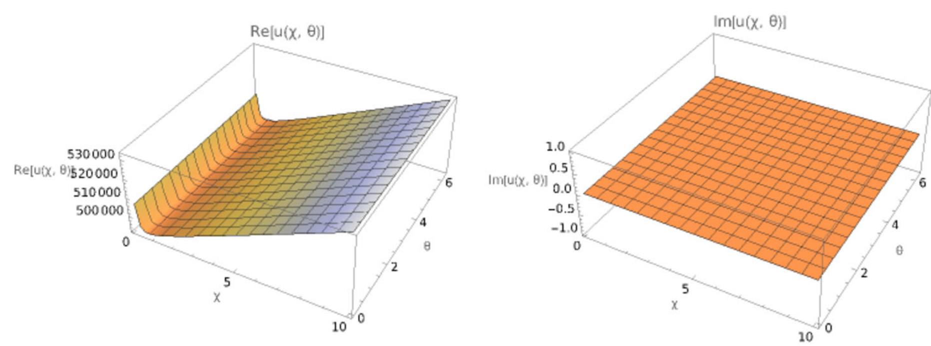

Figure 3 The behavior of *Re*(*u*) and *Im*(*u*)

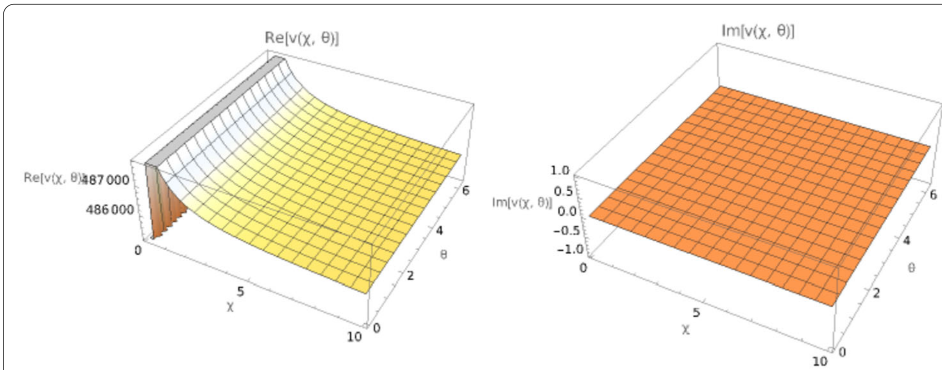

Figure 4 The behavior of *Re*(*v*) and *Im*(*v*)

axis corresponding to χ represents the radial distance from the center of the circular hole, and the corresponding axis of θ represents the angular coordinates around the hole. The plot of Re[$u(\chi,\theta)$] for a porous isotropic magnesium crystal helps visualize the material's response, highlighting areas of stress concentration and weakened stiffness due to porosity, essential for informed material design and application. The imaginary part of the function $u(\chi,\theta)$ is uniform, indicating consistent damping or phase effects throughout the material. This uniformity can be crucial for applications where stable phase characteristics are desired. The plot for the real part of $v(\chi,\theta)$ shows how the tangential displacement varies with χ and θ, highlighting areas of stress concentration and informing material design strategies. The plot for the imaginary part of $v(\chi,\theta)$ is similar to $Im(u(\chi,\theta))$.

8 Conclusion

Graphs representing complex potentials and stress and displacement distributions in a material have many practical applications in various fields of engineering and materials science. They are powerful tools in the analysis and design of materials and structures. They allow a deep understanding of the mechanical behavior of materials, identifying critical points and optimizing the design for superior performance and safety. These techniques are essential in a wide range of industries, from structural and aerospace engineering to bioengineering and scientific research.

Author contributions

D.M.N., I.M.F. and M.M. wrote the main manuscript text and D.M.N.and I.M.F. prepared figures. All authors reviewed the manuscript.

Funding

No funds were used for the development of this manuscript.

Data availability

No datasets were generated or analysed during the current study.

Declarations

Ethics approval and consent to participate

Not applicable.

Competing interests

The authors declare no competing interests.

Received: 11 June 2024 Accepted: 25 September 2024 Published online: 11 October 2024

References

1. Eringen, A.C.: Linear theory of micropolar elasticity. J. Math. Mech. **15**, 909–923 (1966)
2. Eringen, A.C.: Theory of micropolar elasticity. In: Leibowitz, H. (ed.) Fracture, vol. II, p. 622. Academic Press, New York (1968)
3. Eringen, A.C.: Theory of micropolar elasticity. In: Microcontinuum Field Theories. Springer, New York (1999)
4. Cosserat, E., Cosserat, F.: Sur la Théorie des Corps Deformables. Dunod, Paris (1909)
5. Passarella, F.: Some results in micropolar thermoelasticity. Mech. Res. Commun. **23**(4), 349–357 (1996)
6. Moiola, A., Hiptmair, R., Perugia, I.: Plane wave approximation of homogeneous Helmholtz solutions. Z. Angew. Math. Phys. **62**, 809–837 (2011)
7. Ariman, T., Zika, M.J.: On complex potentials in micropolar elasticity. Z. Angew. Math. Mech. **51**(3), 183–188 (1971)
8. Mindlin, R.D.: Complex representation of displacements and stresses in plane strain with couple-stresses. In: Proc. Int. Sympos. on Applications of the Theory of Functions in Continuunm Mechanics, Tbilisi, U.S.S.R, pp. 256–269 (1963)
9. Neagu, D.M., Fudulu, I.M., Marin, M., Öchsner, A.: Wave propagation with two delay times in an isotropic porous micropolar thermoelastic material. Contin. Mech. Thermodyn. **36**, 639–655 (2024)
10. Marin, M.: On existence and uniqueness in thermoelasticity of micropolar bodies. C. R. Acad. Sci. Paris, Sér. II, B **321**(12), 375–480 (1995)
11. Marin, M., Öchsner, A., Bhatti, M.M.: Some results in Moore-Gibson-Thompson thermoelasticity of dipolar bodies. Z. Angew. Math. Mech. **100**(12), Art No. e202000090 (2020)
12. Vlase, S., et al.: Coupled transverse and torsional vibrations in a mechanical system with two identical beams. AIP Adv. **7**(6), Art. No. 065301 (2017)
13. Marin, M., Hobiny, A., Abbas, I.: Finite element analysis of nonlinear bioheat model in skin tissue due to external thermal sources. Mathematics **9**(13), Art. No. 1459 (2021)
14. Marin, M., Fudulu, I.M., Vlase, S.: On some qualitative results in thermodynamics of Cosserat bodies. Bound. Value Probl. **2022**, Art. No. 69 (2022)
15. Marin, M., Vlase, S., Fudulu, I.M., Precup, G.: Effect of voids and internal state variables in elasticity of porous bodies with dipolar structure. Mathematics **9**(21), Art. No. 2741 (2021)

16. Pop, N.: A finite element solution for a three-dimensional quasistatic frictional contact problem. Rev. Roum. Sci. Tech., Sér. Méc. Appl. **42**(1–2), 209–218 (1997)
17. Marin, M., Vlase, S., Fudulu, I.M., Precup, G.: On instability in the theory of dipolar bodies with two-temperatures. Carpath. J. Math. **38**(2), 459–468 (2022)
18. Marin, M., Vlase, S., Neagu, D.: On a composite obtained by a mixture of a dipolar solid with a Moore–Gibson–Thompson media. Bound. Value Probl. **2024**, Art. No. 16 (2024)
19. Marin, M., Vlase, S., Neagu, D., Dominte, L.: On uniqueness and dilatational waves in a porous Cosserat thermoelastic body. J. Umm Al-Qura Univ. Eng. Archit. **15**, 61–66 (2024)
20. Vlase, S., et al.: Analysis of vibration suppression in multi-degrees of freedom systems. Rom. J. Acoust. Vib. **19**(2), 149–156 (2022)

Publisher's Note
Springer Nature remains neutral with regard to jurisdictional claims in published maps and institutional affiliations.